HHS Public Access

Author manuscript

Cellulose (Lond). Author manuscript; available in PMC 2016 August 01.

Published in final edited form as:

Cellulose (Lond). 2015 August 1; 22(4): 2311–2324. doi:10.1007/s10570-015-0651-x.

Modification of Bacterial Cellulose with Organosilanes to Improve Attachment and Spreading of Human Fibroblasts

Siriporn Taokaew[1,2], **Muenduen Phisalaphong**[1], and **Bi-min Zhang Newby**[2,*]

[1]Department of Chemical Engineering, Chulalongkorn University, Bangkok 10330, Thailand
[2]Department of Chemical and Biomolecular Engineering, The University of Akron, Akron, OH, 44325-3906, United States

Abstract

Bacterial Cellulose (BC) synthesized by *Acetobacter xylinum* has been a promising candidate for medical applications. Modifying BC to possess the properties needed for specific applications has been reported. In this study, BCs functionalized by organosilanes were hypothesized to improve the attachment and spreading of Normal Human Dermal Fibroblast (NHDF). The BC gels obtained from biosynthesis were dried by either ambient-air drying or freeze drying. The surfaces of those dried BCs were chemically modified by grafting methyl terminated octadecyltrichlorosilane (OTS) or amine terminated 3-aminopropyltriethoxysilane (APTES) to expectedly increase hydrophobic or electrostatic interactions with NHDF cells, respectively. NHDF cells improved their attachment and spreading on the majority of APTES-modified BCs (~70-80% of area coverage by cells) with more rapid growth (~2.6-2.8× after incubations from 24 to 48h) than on tissue culture polystyrene (~2×); while the inverse results (< 5% of area coverage and stationary growth) were observed on the OTS-modified BCs. For organosilane modified BCs, the drying method had no effect on *in vitro* cell attachment/spreading behaviors.

Keywords

Bacterial cellulose; Modification; Organosilanes; Fibroblasts

Introduction

The trend in wound healing is currently attending to the dressing materials on which the cells can have an excellent cellular response, including cell attachment and proliferation, and form a new tissue if necessary. Basically, dressing materials have to show a biocompatibility, and enhance a major healing process, which requires attachment and proliferation of fibroblasts (Boateng et al. 2008; Velnar et al. 2009). Bacterial cellulose (BC), a biomaterial synthesized by strains of the Gram-negative bacterium *Acetobacter xylinum* (*A. xylinum*), has been reported to exhibit an excellent biocompatibility, good

*Corresponding Author: Bi-min Zhang Newby, Department of Chemical and Biomolecular Engineering, The University of Akron, 200 E. Buchtel Commons, Whitby Hall 101, Akron, Ohio 44325-3906, United States, TEL: +1 330 972-2510, FAX: +1 330 9725856, bimin@uakron.edu.

mechanical properties, and a high water holding capacity (Helenius et al. 2006; Klemm et al. 2001; Svensson et al. 2005). Such unique properties of BC have attracted many *in vitro* and *in vivo* studies in evaluating its biomedical applications including wound dressing (Czaja et al. 2007; Fontana et al. 1990; Helenius et al. 2006; Hoenich 2006; Klemm et al. 2001; Svensson et al. 2005). BC is a highly hydrophilic material capable of absorbing liquid by capillary action through abounding spaces between networks of cellulose fibers (Iguchi et al. 2000; Klemm et al. 2005). It is therefore expected to absorb essential nutrients in the liquid media and consequently enhance cell attachment/proliferation. However, as compared to expensive protein-based materials, BC exhibits low cell attachment and proliferation, especially for fibroblast cells (Roy et al. 1997; Sanchavanakit et al. 2006). It has been reported that a single fibroblast could generate contractile force between underlying substrate and among cells. The force between fibroblasts and BC was weaker than that among the cells themselves, as a result, the cells would round up and be unable to reach confluence on BC (Roy et al. 1997; Sanchavanakit et al. 2006). Thus, modification of BC to improve its ability for fibroblast attachment and proliferation is necessary.

Several modification techniques have been purposed to improve the cellular responses of fibroblast on different materials. The techniques include biopolymer/protein adsorption (Andrade et al. 2010; Cai and Kim 2010; Kim et al. 2010; Zhijiang and Guang 2011), surface modification using gaseous plasma (Pertile et al. 2010; Yang et al. 2002), and with self-assembled monolayers (SAMs) (Curran et al. 2005; Faucheux et al. 2004; Toworfe et al. 2009). A SAM provides an effective chemical modification without affecting the physical and mechanical properties of the underneath bulk materials. Organosilanes are a group of most widely utilized chemicals to form SAMs on the surface. Normally, they are chemically grafted to a hydroxyl-rich surface, including celluloses (Abdelmouleh et al. 2004; Abdelmouleh et al. 2005; Abdelmouleh et al. 2002; Bel-Hassen et al. 2008; Belgacem et al. 2010; Brochier Salon et al. 2005; Brochier Salon and Belgacem 2010; Salon et al. 2007; Tonoli et al. 2013), using their head groups (see Fig. 1), while the desired terminal groups (i.e., functional groups) are pointing to the surrounding to interact with cells/proteins (Arima and Iwata 2007; Faucheux et al. 2004; Luk et al. 2000; McClary et al. 2000). Depending on the terminal groups, enhanced interactions could result. Since the BC surface possesses abundance of hydroxyl groups, which could covalently bond with hydrolyzed organosilane molecules, making it possible to modify BC surfaces with organosilanes.

In this study, we intended to evaluate attachment, spreading and growth of normal human dermal fibroblasts (NHDF) on BCs modified by two types of organosilanes. We hypothesized that cell attachment and spreading could be improved by introducing methyl (CH_3)-terminated octadecyltrichlorosilane (OTS), to enhance hydrophobic interactions, or amino (NH_2)-terminated 3-aminopropyltriethoxysilane (APTES), to enhance electrostatic interactions, on the surface of BCs. Surfaces of modified BCs were characterized by Scanning Electron Microscopy (SEM) for surface morphology, contact angle measurement for surface wettability and estimating surface energy, and X-ray Photoelectron Spectroscopy (XPS) for surface chemistry. Cell behaviors of NHDF cultured on BCs surface modified with these two organosilanes were evaluated by Live/Dead assay, MTT assay and SEM.

Experimental details

Materials

All chemicals were purchased from Sigma-Aldrich, Inc., MO, USA unless otherwise noted. Normal human dermal fibroblasts derived from adult skin (NHDF; CC-2511) and fibroblast growth medium (FGM™-2 BulletKit™), containing 0.1% of 1 mg/ml of human recombinant fibroblast growth factor, 0.1% of 5 mg/ml of Insulin, 0.1% of 50 mg/ml of antibiotics (Gentamicin and AmphotericinB), and 2% fetal bovine serum, were purchased from Lonza Walkersville, Inc., MD, USA. *Acetobacter xylinum* bacterial strain AGR60 was supplied by Pramote Thammarad, the Institute of Research and Development of Food Product, Kasetsart University, Bangkok, Thailand.

Production of bacterial cellulose

Bacterial cellulose hydrogel were produced by cultivation of *A. xylinum* in coconut-based medium supplemented with 5% w/v of sucrose (Ajax Finechem, Australia), and 0.5% w/v of ammonium sulfate (Ajax Finechem, Australia). The culture medium was adjusted to an acidic pH of 4-5 by using acetic acid (QRec, New Zealand). After autoclaving at 110°C for 5 min, 75-ml of cooled sterile medium was then aseptically transferred to a sterile 14.5-cm. diameter Petri-dish, and 5% v/v of the pre-culture of *A. xylinum* was thoroughly mixed. The incubation was performed statically under ambient condition (29 ± 3 °C, 1 atm, and 70-80% humidity) for 7 days. After BC pellicles formed in to the desired thickness (∼ 1 cm.), they were purified by treating with 1% w/v of NaOH (Ranken, India) for 24 h, and neutralizing with copious deionized (DI) water. The pellicles were stored in DI water at 4 °C prior to use. To prepare for further surface modification, BC were cut into ∼ 1×1 cm^2 pieces before drying. Then they were dried by either ambient-air drying on glass slide for 48 h or freeze drying for 24 h. For freeze drying, BCs were frozen in liquid nitrogen for 2 h before immediately loading the frozen sample in to a chamber of a freeze dryer (VirTis-SP Scientific sentry 2.0, USA). The freezing drying process was run at a condenser temperature of -80 °C under high vacuum.

Surface modification by organosilanes

Surfaces of air dried and freeze dried BCs were modified by using 3-aminopropyltriethoxysilane (APTES) or octadecyltrichlorosilane (OTS) to allow amine or methyl groups on their surfaces, respectively. The procedure of modification is illustrated in Fig. 1. APTES and OTS were individually diluted to 1 wt.% in HPLC grade hexane, and then 0.2 mL of either solution was dispersed to a circular area of ∼ 2 cm^2 on a polystyrene Petri dish with a diameter of 3.5 cm. BCs were subsequently brought down into contact with the spread solution for 30 sec at room temperature. For removing excess organosilanes on BCs, they were tapped on a Petri dish containing a thin layer (∼ 0.2 mm) of fresh hexane for a few times, blown dried with a stream of nitrogen gas, and afterwards annealed at 65 °C inside an oven for an hour. Additionally, glass slides, used to compare with results on BCs, were cut into ∼ 1×1 cm^2, cleaned with a fresh piranha solution (Weisbecker et al. 1996) followed by oxidization using UV/O_3 for 6 min, and then were functionalized following the method described above.

Characterizations

For Surface morphology, Scanning Electron Microscopy (SEM) was performed using JEOL JSM- 5410LV SEM (Japan) to examine the surface morphologies of typical and modified BCs. The dried samples were sputtered with ~200 Å of gold in a Balzers-SCD 040 sputter coater (Liechtenstein). The images were immediately viewed at a magnification of 10,000× and an accelerating voltage of 15kV.

For surface wettability, contact angles of water (W) on the unmodified and modified surfaces were measured in ambient condition using a Rame-Hart 100-00 contact angle goniometer (USA). The liquid was dispersed from a microliter syringe onto ten random locations of the surface. Images of static contact angles were recorded using the WinTV software (Version 7.0.30237, Hauppauge computer works) and measured using Image J (Version 1.43t, National Institute of Health).

For surface chemistry, X-ray photoelectron spectroscopy (XPS) was carried out using a Kratos Axis Ultra spectrometer (UK) equipped with a monochromatic Al Kα X-ray source (1486.6 eV). The analyzer was operated under 15kV, 150W, 10 mA, an ultra-high vacuum pressure (~ 10^{-9} Torr) and a 90° take-off angle. The survey and high-resolution scans (spot size of 700×300 μm) were provided in hybrid mode with pass energies of 160 and 40 eV, respectively. Background subtraction, peak integration, fitting, and chemical analysis for C1s, O1s, and N1s individual spectra were acquired by Vision2 software (UK). A peak of carbon atoms with a single bond (C-C) in C1s spectra at 285.0 eV was used to calibrate the binding energy scale.

Cell study

For culture NHDF on BCs and glass slides, NHDF cells (passage 10-15) were grown to 90-95% confluence in T75 culture flask pre-coated with 0.1 % (w/v) of gelatin. The cells were harvested based on the manufacturer's protocol for detachment to obtain single cells. 50 μl containing 5×10^4 cells in growth medium was plated on a BC sample, a piece of glass slide or tissue culture polystyrene (TCP), which were controlled to a culture area of ~ 8×8 mm^2. 1 ml of fibroblast growth medium was then gently pipetted to each well of 24-well plate, where each of the samples was placed in, to submerge the sample containing cells. The incubation was performed at 37°C in humidified atmosphere with 5% CO_2 for 24 and 48 h.

For cell attachment and spreading evaluations, fluorescence and electron microscopies were used to evaluate the attachment and spreading of NHDF cells. For fluorescence microscopy, live cells were stained with fluorescein diacetate (FDA). The stained cells were gently rinsed twice with ~ 500 μL of phosphate buffer (pH 7.4) and immediately visualized by an Olympus IX70 microscope with AmScope MT software (version 3.0.0.0) using a 10× objective (i.e., with a magnification of 100×). Images of cells spreading over random sections of each sample were quantified by color range mode of Adobe Photoshop CS5 (Version 12.0.3×32). Briefly, the image size was adjusted to 6×8 cm^2 or 354×472 pixels/image (a resolution of 150 p.p.i.). The green color of NHDF was detected and read in the unit of pixel. The pixels of spreading cells were converted into percentage of area coverage

as followed: $\%area\ coverage\ by\ cells = \frac{P_{green}}{P_{total}} \times 100\%$, where P_{green} and P_{total} denote pixels of area coverage by cells showing green and pixels of total area of an image, respectively. For a higher magnification, NHDF cells cultured on BCs for 48h were examined by SEM using a magnification of 1,000×. The attached cells were fixed in 4 % (v/v) of paraformaldehyde solution in phosphate buffer for 36 h, washed with distilled water for several times, and dehydrated with a series of graded ethanol (10, 30, 50, 70, 90 % (v/v), and absolute). The fixed cells were dried in Tousimis Samdri-780 liquid CO_2 critical point dryer (USA) and uniformly coated with a thin layer of gold before scanning at an accelerating voltage of 15kV.

For cell viability studies, MTT assay (Invitrogen) was employed, and absorbance at the wavelength of 570 nm was measured by a microplate reader (Tecan Infinite® M200, Switzerland). After 24 and 48 h of incubations, samples were relocated to the individual wells of a new 24-well plate. 1 ml of MTT solution was gently added to those wells with samples and without samples (blank reference). An absorbance value of blank was subtracted from the values of samples before normalizing by the absorbance of TCP after 24 h of incubation. The results were expressed as relative cell number as followed:

$Relative\ cell\ number = \frac{Ab_{sample} - Ab_{blank}}{Ab_{TCP@24h} - Ab_{blank}}$, where Ab_{sample}, Ab_{blank}, and $Ab_{TCP@24h}$ represent absorbance values of sample of each period of incubation, blank of each period of incubation, and tissue culture polystyrene at 24 h of incubation, respectively. Hence, the cell number in tissue culture polystyrene after 24 h of incubation was defined as 1.0. The experiments were independently carried out in triplicate.

Statistical analysis

The obtained data were expressed as an average from at least three experiments and statistically analyzed by student *t*-test: two-sample assuming equal variances. The differences were considered significant at the level of $p<0.05$.

Results and Discussion

Surface morphology

After dehydration using either air drying or freeze drying, the average fiber diameter of unmodified air dried BC (Fig. 2A) and freeze dried BC (Fig. 2D) was in a similar range (100-300 nm) as seen from the microscopic view using SEM at a magnification of 10,000×. The fiber network of air dried BC sheet was much denser than that of freeze dried BC. This was likely due to the slow-drying caused the collapse structure of BC in the thickness direction (Taokaew et al. 2014). After modifying with organosilanes, changes of surface morphologies were discerned on surfaces of the OTS-modified air dried BCs (Fig. 2B), the APTES-modified air dried BCs (Fig. 2C), and the APTES-modified freeze dried BCs (Fig. 2F) as compared to those of unmodified samples. The slightly decreased pore size, defining as the reduced spaces between fibers, was observed on the surface of the OTS-modified freeze dried BC (Fig. 2E), while the fiber size was not considerably different from that of the unmodified one. In this case, pores of BC were presumably blocked by a layer of OTS

attached onto the BC surface. The blockage depended on many factors, for instance, the initial concentration of organosilane solution, the large molecular size and the large functional head groups along with the molecular configuration of organosilane (Maria Chong et al. 2004; Zhao et al. 1997). By estimating from Fig. 2D, the pores distributed on the freeze dried BC were approximately 0.3-2.5 μm, which were possibly blocked by aggregates of relatively large OTS molecules (the molecular size of OTS is ∼ 0.50 nm × 2.60 nm (Maria Chong et al. 2004)) at the prepared concentration (1 wt.% OTS/hexane). This could cause the minor change of surface morphology besides functionalizing the BC surfaces with hydrophobic methyl groups after being modified. Unlike the OTS-modified samples, fiber diameter and pore structure of the APTES-modified air dried (Fig. 2C) and freeze dried BCs (Fig. 2F) did not obviously differ from those of unmodified samples. Pore dimension of BC was not largely disturbed by the shorter and smaller APTES molecules (the molecular size of APTES is ∼ 0.25 nm × 0.80 nm) (Chiang et al. 1980; Rodriguez et al. 2014; Stephen Caravajal et al. 1988).

Surface wettability

Contact angle is common for characterizing surface wettability along with estimating surface energy of a solid (Bain et al. 1989; Chaudhury 1996; Owens and Wendt 1969; Żenkiewicz 2007). Apparent contact angles of water on the resulting BC surfaces are listed in Table 1. While contact angles for porous structures might not truly represent the surface wettability of the material, they could still provide a relative comparison on the extent of wettability and a quick assessment on whether or not a surface might have been functionalized. Water contact angles indicated some diminution of hydrophilicity in the air dried BC (water contact angle of 56.3 ± 8.0°) as compared to the freeze dried BC, which mostly remained the dimension and pore structure from those of never dried BCs. This could be due to some rearrangements of fiber structure resulting in porosity reduction during the slow evaporation process of air-drying (Taokaew et al. 2014). The freeze dried BC remained highly hydrophilic with water droplets quickly absorbed into the sample. After modifying with OTS, an increased in water contact angle was observed, indicating that some hydrophobic functional groups (methyl group in this study) presented on the dried BCs. The water contact angles of the resulting OTS-modified air dried and OTS-modified freeze dried BCs valued at 90.7 ± 5.1° and 112.4 ± 9.5°, respectively. For modification with APTES, the results were not considerably different from those without modification. This could be explained by the similar surface morphology and termination of BC surfaces with polar/hydrophilic functional groups (hydroxyl in BC vs. amine in APTES-modified BC). Apparently, the APTES-modified air dried BC exhibited a slightly less hydrophilicity with a water contact angle of 67.6± 2.3°, while the APTES-modified freeze-dried BC appeared completely wetted as the non-modified freeze dried BC.

Surface chemistry

The surface composition of the organosilane-modified BCs was determined by XPS. The survey scan spectra initially showed the relevant atoms distributed on BC surfaces (Table 2). The main detectable elements in all samples were carbon (C) and oxygen (O). Oxygen to carbon ratios (O/C) of BC undergone air drying and freeze drying were similar (0.92 and 0.88, respectively), which were close to the theoretical O/C ratio of pure cellulose (∼ 0.8)

(Johansson et al. 1999; Johansson and Campbell 2004; Sevilla and Fuertes 2009). A trace amount of nitrogen (N), with nitrogen to carbon ratio (N/C) less than 0.01, also appeared on the typical dried BC, which was likely attributed to some residual proteins from BC-producing bacteria. After modification by OTS, with the addition of OTS molecules that contain long hydrocarbon chain, the O/C ratios of the modified air dried and freeze dried BCs slightly decreased from that of the unmodified BC to 0.74 and 0.49, respectively, while N/C ratios remained very low. For the surfaces of air dried and freeze dried BCs modified by APTES, nitrogen amount increased as indicated by the N/C ratios increasing to 0.05 and 0.02, respectively, demonstrating that APTES molecules (containing – NH_2 terminal group) were presented on BC. But, their O/C ratios (0.83 and 0.88 respectively) were basically not affected.

To provide more details on the chemistry of the sample, high-resolution spectra were obtained, and the broad C1s peak was deconvoluted into peaks associated with an un-oxidized carbon atom (C-H, C-C, or C=C) at the binding energy of ∼ 285.0 eV, a carbon atom bound singly to an oxygen atom (C-O) and doubly to an oxygen atom (C=O) (or two single bonds: OC-O) at the binding energies of ∼ 286.5 eV and ∼ 288.5 eV, respectively (Barazzouk and Daneault 2012; Sevilla and Fuertes 2009). The predominant carbon composition (∼60-70%) appeared in non-modified air dried and freeze dried BC samples was C-O, referring to the hydroxyl groups linked carbon (Fig. 3 A and D). It was observed that the C-C peaks were the main peaks of the OTS-modified air dried and freeze dried BCs (Fig. 3 B and E), associated with the long hydrocarbon chain of OTS. The C-C composition increased from ∼11-19% of non-modified BCs to ∼52-91% for the OTS modified BCs. The shorter chain of APTES caused some change of carbon atom linkage for the APTES-modified air dried and freeze dried BCs (Fig. 3 C and F). The percent composition of C-C increased to ∼26% and ∼37%, respectively, for the APTES-modified air dried and freeze dried BCs, while the percent composition of C-O reduced to ∼50 - 60%. For N1s scans, negligible signal of nitrogen peaks presented before and after the modification by OTS, but the peaks for APTEs modified samples were much more obvious. The APTES-modified air dried and freeze dried BCs exhibited two peaks at the binding energy of ∼399 and 400 eV, which were attributed to free amine (H_2N-C) and amide (O=C-N-C) (Barazzouk and Daneault 2012; Jewett et al. 2011; Pertile et al. 2010), and had a percent composition of 76-85% and 15-24%, respectively (Fig. 3 G and H).

Cell attachment and spreading studies

From fluorescent microscopy, green-stained NHDF cells attaching and spreading over sections of unmodified and organosilane-modified air dried BCs, freeze dried BCs, and glass surfaces were imaged (Fig. 4A). Subsequently, the % area covered by cells at several random locations of a sample was quantified and the results were summarized in Fig. 4B. On the air-dried BC, after incubation for 48 h, some rounded attached cells were observed (Fig. 4 (A1)), and the cells covered ∼ 7.6 % of the total area (Fig. 4B). For 48 h of incubation, more cells attached and spread on the freeze dried BC (Fig. 4 A4) and on the glass slide (Fig. 4 A7) with ∼ 58.5% and ∼ 77.5%, respectively, of area coverage by cells. After modification with OTS, a methyl (-CH_3) terminated organosilane to increase the surface hydrophobicity, only non-spread rounded individual NHDF cells were noticed on

the OTS-modified air-dried BCs (Fig. 4 A2), few spread cells appeared on the OTS-modified freeze dried BC (Fig. 4 A5), and some cells on the OTS-modified glass slide (Fig. 4 A8). As compared to those on the unmodified samples possessing hydroxyl groups in nature, the cell numbers on the OTS-modified samples were much less, and the % area coverage by cells on the OTS-modified surface was less than 10%. One potential cause for the lower number of cells attaching and spreading on the OTS modified samples could be the faster adsorption of bovine serum albumin (BSA) on the OTS surface due to the enhanced hydrophobic interactions, and the BSA layer might deter the attachment of NHDF cells. In spite of protein adhesiveness guided by hydrophobic interactions from the hydrophobic surface (Healy et al. 1996; Norde and Lyklema 1991), the adsorbed proteins on the hydrophobic surface might not appear in the appropriate configuration or had been denatured (Webb et al. 1998), consequently cell attachment and spreading could not be promoted (Baugh and Vogel 2004; Faucheux et al. 2004; Roach et al. 2005).

Another factor to favor cell attachment/spreading could be surface charge, which would alter the electrostatic interactions (Curtis 1964; Webb et al. 1998). The surface modification was reported to enhance physisorption of extracellular matrix proteins via electrostatic interactions (Ratner 1993). Positive charges of amine groups were introduced by modifying the samples with APTES (zeta potential of silica particles modified with APTES was measured to be 18 ± 2 mV), an organosilane terminated with amine ($-NH_2$). Spread NHDF cells covering majority of the surface was observed on these samples. The cells were found to be over-crowded and more spread on the APTES- modified air-dried BC (Fig. 4 A3); even more cells, appeared to form a multilayer and even slightly detached from the surface, likely due to the steady state culture of the confluent colonies, were noticed on the APTES-modified freeze dried BC (Fig. 4 A6), and on the APTES-modified glass slide (Fig. 4 A9). It was reported that when the confluence or the stead state culture was attained, those confluent colonies were replaced by divided cells which proliferated in the basal layer and underwent detachment by themselves from the surface (Arisaka et al. 2013; Green 1977). % area coverage by cells was ∼71.2%, ∼75.7%, and ∼84.7%, respectively, on the APTES-modified air dried BC, the APTES-modified freeze dried BC, and the APTES-modified glass slide. % area coverage by cells on the APTES-modified BCs were improved by ∼ 30-40× as compared to those on the OTS-modified BCs. Positively-charged surfaces have been reported to enhance affinity to cells because of electrostatic interactions. The initial attachment and distribution of cells occurred due to the positive charge of amine-terminated surface, presumably associating with the negatively-charged cell surface (Healy et al. 1996; Lee et al. 1997; Soekarno et al. 1993). The over-crowed cells on the surface, which would be beneficial for tissue replacement or wound dressing application, have been reported (Boateng et al. 2008).

NHDF cells cultured on the unmodified and the APTES-modified BCs after 48 h were examined in more details, as seen in Fig. 5, using SEM. The SEM images revealed that some attachment and spreading of the NHDF cells on the unmodified air dried and freeze dried BCs (Fig. 5 A and C). The enhanced spreading indicated by lamellipodia of cells on the APTES-modified air dried and freeze dried BCs (Fig. 5 B and D) was noticed as compared to the unmodified BCs. Moreover, the cells especially on the APTES-modified freeze dried BCs had better interactions to adjacent cells.

Cell viability studies

Results of MTT assay (Fig. 6) confirmed that NHDF cells after incubations for 24 and 48 h on the unmodified and the organosilane-modified surfaces were viable. Relative cell number was used as a comparable parameter for defining how many cells could survive as compared to those cultivated on TCP, which is generally applied as a control or a reference in most studies. In this study, the ratio of cell number on tissue culture polystyrene after 24 h of incubation was defined as 1.0.

As seen in Fig. 6, increases in ratios of the relative cell number from 24 to 48 h of incubation were noticed on glass slides (from ∼0.9 to ∼1.5), unmodified BCs (from ∼0.3 to ∼0.4 and from ∼0.5 to ∼0.9 for air dried and freeze dried BCs, respectively), and the APTES-modified BCs (from ∼0.5 to ∼1.3 and from ∼0.5 to ∼1.4 for air dried and freeze dried BCs, respectively). The ratios of relative cell number of the culture on TCP (from 1.0 to ∼2.0) were greater than those on the prepared BCs and glass slides. The relative cell numbers on the APTES-modified BCs raised by ∼2.6 - ∼2.8× during the latter period (from 24 h to 48 h) of incubation, which was a more rapid growth than that on TCP (∼2×). This could imply that the more rapid growth of cells were triggered by a good cell adhesion, specially good interactions between cells and underlying material in the first phase of cellular response (Anselme 2000). For most cell types, survival of cells including cell growth and function induced by integrins, proteins that mechanically linked cells to the substrate. Without this focal adhesion via a layer of proteins, cells undergo programmed cell death (Izzard and Lochner 1976; Ruoslahti and Reed 1994; Singhvi et al. 1994). In the case of the OTS-modified BCs, only slight dissimilarities of relative cell numbers (less than 0.5) between the two periods of incubations were noticed.

Conclusions

In this framework, we hypothesized that the modification of dried BCs using organosilanes of OTS and APTES would enhance hydrophobic and electrostatic interactions, respectively, between fibroblast cells and BC surfaces with the goal of improving NHDF cell attachment and proliferation. Surface morphology of the OTS-modified air dried and freeze dried BCs appeared minor changes; while that of the APTES-modified air dried and freeze dried BCs as well as the typical non-modified BCs were apparently analogous. When modified by OTS, BCs achieved enhanced surface hydrophobicity with greater water contact angles due to the presence of methyl groups. The positively-charged APTES did not greatly affect the wettability of the BC surfaces after they were modified with APTES, as compared to those of non-modified BCs. Opposed to our expectation, cell attachment and spreading appeared worse on the OTS-modified air dried and freeze dried BCs. However, much more enhanced cell attachment and proliferation were achieved on the APTES modified BCs, indicating, as compared to hydrophobic interactions, electrostatic interactions was better in promoting fibroblast cell adhesion on a surface. This was judged by the greater overall cell shape, % cell coverage, and relative viable cell number. The well-spread cells reached the confluence on the APTES-modified BCs within 48 h, with ∼ 80% of area coverage by viable cells. Overall, the similar cellular response on BCs dried differently implied that drying of BC was less critical towards cell adhesion and spreading on the organosilane-modified surfaces, the

resulting surface properties (wettability, charge), on the other hand, were crucial. The results from this study suggest that BC surface modified by APTES would be beneficial to promote cell growth for wound dressing applications, while BCs modified by OTS could be a candidate for anticancer/antibacterial applications.

Acknowledgments

The authors are grateful for the financial support from the Royal Golden Jubilee Ph.D program from the Thailand Research Fund and the Ratchadaphiseksomphot Endowment Fund of Chulalongkorn University for Project RES560530044-AM and Postdoctoral Fellowship; as well as the National Institutes of Health, the National Institute of General Medical Sciences under award number 1R15GM097626-01A1 (to BMZN).

References

Abdelmouleh M, Boufi S, Belgacem MN, Duarte AP, Ben Salah A, Gandini A. Modification of cellulosic fibres with functionalised silanes: Development of surface properties. Int J Adhes Adhes. 2004; 24:43–54.

Abdelmouleh M, Boufi S, Belgacem MN, Dufresne A, Gandini A. Modification of cellulose fibers with functionalized silanes: Effect of the fiber treatment on the mechanical performances of cellulose-thermoset composites. J Appl Polym Sci. 2005; 98:974–984.

Abdelmouleh M, Boufi S, Salah AB, Belgacem MN, Gandini A. Interaction of silane coupling agents with cellulose. Langmuir. 2002; 18:3203–3208.

Andrade FK, Moreira SMG, Domingues L, Gama FMP. Improving the affinity of fibroblasts for bacterial cellulose using carbohydrate-binding modules fused to RGD. J Biomed Mater Res A. 2010; 92:9–17. [PubMed: 19165790]

Anselme K. Osteoblast adhesion on biomaterials. Biomaterials. 2000; 21:667–681. [PubMed: 10711964]

Arima Y, Iwata H. Effect of wettability and surface functional groups on protein adsorption and cell adhesion using well-defined mixed self-assembled monolayers. Biomaterials. 2007; 28:3074–3082. [PubMed: 17428532]

Arisaka Y, Kobayashi J, Yamato M, Akiyama Y, Okano T. Switching of cell growth/detachment on heparin-functionalized thermoresponsive surface for rapid cell sheet fabrication and manipulation. Biomaterials. 2013; 34:4214–4222. [PubMed: 23498894]

Bain CD, Troughton EB, Tao YT, Evall J, Whitesides GM, Nuzzo RG. Formation of monolayer films by the spontaneous assembly of organic thiols from solution onto gold. J Am Chem Soc. 1989; 111:321–335.

Barazzouk S, Daneault C. Amino Acid and Peptide Immobilization on Oxidized Nanocellulose: Spectroscopic Characterization. Nanomaterials. 2012; 2:187–205.

Baugh L, Vogel V. Structural changes of fibronectin adsorbed to model surfaces probed by fluorescence resonance energy transfer. J Biomed Mater Res A. 2004; 69:525–534. [PubMed: 15127399]

Bel-Hassen R, Boufi S, Salon MCB, Abdelmouleh M, Belgacem MN. Adsorption of silane onto cellulose fibers. II. The effect of pH on silane hydrolysis, condensation, and adsorption behavior. J Appl Polym Sci. 2008; 108:1958–1968.

Belgacem MN, Salon-Brochier MC, Krouit M, Bras J. Recent advances in surface chemical modification of cellulose fibres. J Adhes Sci Technol. 2010; 25:661–684.

Boateng JS, Matthews KH, Stevens HNE, Eccleston GM. Wound healing dressings and drug delivery systems: A review. J Pharm Sci. 2008; 97:2892–2923. [PubMed: 17963217]

Brochier Salon MC, Abdelmouleh M, Boufi S, Belgacem MN, Gandini A. Silane adsorption onto cellulose fibers: Hydrolysis and condensation reactions. J Colloid Interface Sci. 2005; 289:249–261. [PubMed: 15907861]

Brochier Salon MC, Belgacem MN. Competition between hydrolysis and condensation reactions of trialkoxysilanes, as a function of the amount of water and the nature of the organic group. Colloids Surf Physicochem Eng Aspects. 2010; 366:147–154.

Cai Z, Kim J. Bacterial cellulose/poly(ethylene glycol) composite: Characterization and first evaluation of biocompatibility. Cellulose. 2010; 17:83–91.

Chaudhury MK. Interfacial interaction between low-energy surfaces. Mater Sci Eng R. 1996; 16:97–159.

Chiang CH, Ishida H, Koenig JL. The structure of γ-aminopropyltriethoxysilane on glass surfaces. J Colloid Interface Sci. 1980; 74:396–404.

Curran JM, Chen R, Hunt JA. Controlling the phenotype and function of mesenchymal stem cells in vitro by adhesion to silane-modified clean glass surfaces. Biomaterials. 2005; 26:7057–7067. [PubMed: 16023712]

Curtis ASG. The mechanism of adhesion of cells to glass: A Study by interference reflection microscopy. J Cell Biol. 1964; 20:199–215. [PubMed: 14126869]

Czaja WK, Young DJ, Kawecki M, Brown RM Jr. The future prospects of microbial cellulose in biomedical applications. Biomacromolecules. 2007; 8:1–12. [PubMed: 17206781]

Faucheux N, Schweiss R, Lützow K, Werner C, Groth T. Self-assembled monolayers with different terminating groups as model substrates for cell adhesion studies. Biomaterials. 2004; 25:2721–2730. [PubMed: 14962551]

Fontana J, et al. Acetobacter cellulose pellicle as a temporary skin substitute. Appl Biochem Biotechnol. 1990:24–25. 253–264.

Green H. Terminal differentiation of cultured human epidermal cells. Cell. 1977; 11:405–416. [PubMed: 302145]

Healy KE, Thomas CH, Rezania A, Kim JE, McKeown PJ, Lom B, Hockberger PE. Kinetics of bone cell organization and mineralization on materials with patterned surface chemistry. Biomaterials. 1996; 17:195–208. [PubMed: 8624396]

Helenius G, Bäckdahl H, Bodin A, Nannmark U, Gatenholm P, Risberg B. In vivo biocompatibility of bacterial cellulose. J Biomed Mater Res A. 2006; 76:431–438. [PubMed: 16278860]

Hoenich N. Cellulose for medical aplications: past, present, and future. Bioresources. 2006; 1:270–280.

Iguchi M, Yamanaka S, Budhiono A. Bacterial cellulose-a masterpiece of nature's arts. J Mater Sci. 2000; 35:261–270.

Izzard CS, Lochner LR. Cell to substrate contacts in living fibroblasts. An interference reflexion study with an evaluation of the technique. J Cell Sci. 1976; 21:129–159. [PubMed: 932106]

Jewett S, Zemlyanov D, Ivanisevic A. Adsorption of Mixed Peptide/Thiol Adlayers on InAs: Assessment of Different Functionalization Strategies Using X-ray Photoelectron Spectroscopy. J Phys Chem C. 2011; 115:14244–14252.

Johansson LS, Campbell JM, Koljonen K, Stenius P. Evaluation of surface lignin on cellulose fibers with XPS. Appl Surf Sci. 1999:144–145. 92–95.

Johansson LS, Campbell JM. Reproducible XPS on biopolymers: Cellulose studies. Surf Interface Anal. 2004; 36:1018–1022.

Kim J, Cai Z, Chen Y. Biocompatible bacterial cellulose composites for biomedical application. J Nanotech Eng Med. 2010; 1:011006–011012.

Klemm D, Heublein B, Fink HP, Bohn A. Cellulose: Fascinating Biopolymer and Sustainable Raw Material. Angew Chem Int Ed. 2005; 44:3358–3393.

Klemm D, Schumann D, Udhardt U, Marsch S. Bacterial synthesized cellulose — artificial blood vessels for microsurgery. Prog Polym Sci. 2001; 26:1561–1603.

Lee JH, Lee JW, Khang G, Lee HB. Interaction of cells on chargeable functional group gradient surfaces. Biomaterials. 1997; 18:351–358. [PubMed: 9068898]

Luk YY, Kato M, Mrksich M. Self-assembled monolayers of alkanethiolates presenting mannitol groups are inert to protein adsorption and cell attachment. Langmuir. 2000; 16:9604–9608.

Maria Chong AS, Zhao XS, Kustedjo AT, Qiao SZ. Functionalization of large-pore mesoporous silicas with organosilanes by direct synthesis. Microporous Mesoporous Mater. 2004; 72:33–42.

McClary KB, Ugarova T, Grainger DW. Modulating fibroblast adhesion, spreading, and proliferation using self- assembled monolayer films of alkylthiolates on gold. J Biomed Mater Res. 2000; 50:428–439. [PubMed: 10737886]

Norde W, Lyklema J. Why proteins prefer interfaces. J Biomater Sci Polym Ed. 1991; 2:183–202. [PubMed: 1854684]

Owens DK, Wendt RC. Estimation of the surface free energy of polymers. J Appl Polym Sci. 1969; 13:1741–1747.

Pertile RAN, Andrade FK, Alves C Jr, Gama M. Surface modification of bacterial cellulose by nitrogen-containing plasma for improved interaction with cells. Carbohydr Polym. 2010; 82:692–698.

Ratner BD. Plasma deposition for biomedical applications: A brief review. J Biomater Sci Polym Ed. 1993; 4:3–11. [PubMed: 1463698]

Roach P, Farrar D, Perry CC. Interpretation of protein adsorption: Surface-induced conformational changes. J Am Chem Soc. 2005; 127:8168–8173. [PubMed: 15926845]

Rodriguez GA, Ryckman JD, Jiao Y, Weiss SM. A size selective porous silicon grating-coupled Bloch surface and sub-surface wave biosensor. Biosens Bioelectron. 2014; 53:486–493. [PubMed: 24211462]

Roy P, Petroll WM, Cavanagh HD, Chuong CJ, Jester JV. Anin VitroForce Measurement Assay to Study the Early Mechanical Interaction between Corneal Fibroblasts and Collagen Matrix. Exp Cell Res. 1997; 232:106–117. [PubMed: 9141627]

Ruoslahti E, Reed JC. Anchorage dependence, integrins, and apoptosis. Cell. 1994; 77:477–478. [PubMed: 8187171]

Salon MCB, Gerbaud G, Abdelmouleh M, Bruzzese C, Boufi S, Belgacem MN. Studies of interactions between silane coupling agents and cellulose fibers with liquid and solid-state. NMR Magn Reson Chem. 2007; 45:473–483. [PubMed: 17431857]

Sanchavanakit N, Sangrungraungroj W, Kaomongkolgit R, Banaprasert T, Pavasant P, Phisalaphong M. Growth of Human Keratinocytes and Fibroblasts onBacterial Cellulose Film. Biotechnol Prog. 2006; 22:1194–1199. [PubMed: 16889398]

Sevilla M, Fuertes AB. The production of carbon materials by hydrothermal carbonization of cellulose. Carbon. 2009; 47:2281–2289.

Singhvi R, Stephanopoulos G, Wang DIC. Effects of substratum morphology on cell physiology. Biotechnol Bioeng. 1994; 43:764–771. [PubMed: 18615800]

Soekarno A, Lom B, Hockberger PE. Pathfinding by neuroblastoma cells in culture is directed by preferential adhesion to positively charged surfaces. Neuroimage. 1993; 1:129–144. [PubMed: 9343564]

Stephen Caravajal G, Leyden DE, Quinting GR, Maciel GE. Structural characterization of (3-aminopropyl)triethoxysilane-modified silicas by silicon-29 and carbon-13 nuclear magnetic resonance. Anal Chem. 1988; 60:1776–1786.

Svensson A, Nicklasson E, Harrah T, Panilaitis B, Kaplan DL, Brittberg M, Gatenholm P. Bacterial cellulose as a potential scaffold for tissue engineering of cartilage. Biomaterials. 2005; 26:419–431. [PubMed: 15275816]

Taokaew S, Phisalaphong M, Zhang Newby BM. In vitro behaviors of rat mesenchymal stem cells on bacterial celluloses with different moduli. Mater Sci Eng C. 2014; 38:263–271.

Tonoli GHD, Belgacem MN, Siqueira G, Bras J, Savastano H Jr, Rocco Lahr FA. Processing and dimensional changes of cement based composites reinforced with surface-treated cellulose fibres. Cem Concr Compos. 2013; 37:68–75.

Toworfe GK, Bhattacharyya S, Composto RJ, Adams CS, Shapiro IM, Ducheyne P. Effect of functional end groups of silane self-assembled monolayer surfaces on apatite formation, fibronectin adsorption and osteoblast cell function. J Tiss Eng Regen Med. 2009; 3:26–36.

Velnar T, Bailey T, Smrkolj V. The wound healing process: An overview of the cellular and molecular mechanisms. J Int Med Res. 2009; 37:1528–1542. [PubMed: 19930861]

Webb K, Hlady V, Tresco PA. Relative importance of surface wettability and charged functional groups on NIH 3T3 fibroblast attachment, spreading, and cytoskeletal organization. J Biomed Mater Res. 1998; 41:422–430. [PubMed: 9659612]

Weisbecker CS, Merritt MV, Whitesides GM. Molecular Self-Assembly of Aliphatic Thiols on Gold Colloids. Langmuir. 1996; 12:3763–3772.

Yang J, Bei J, Wang S. Improving cell affinity of poly (D,L-lactide) film modified by anhydrous ammonia plasma treatment. Polym Adv Technol. 2002; 13:220–226.

Żenkiewicz M. Comparative study on the surface free energy of a solid calculated by different methods. Polym Test. 2007; 26:14–19.

Zhao XS, Lu GQ, Whittaker AK, Millar GJ, Zhu HY. Comprehensive Study of Surface Chemistry of MCM-41 Using 29Si CP/MAS NMR, FTIR, Pyridine-TPD and TGA. J Phys Chem B. 1997; 101:6525–6531.

Zhijiang C, Guang Y. Bacterial cellulose/collagen composite: Characterization and first evaluation of cytocompatibility. J Appl Polym Sci. 2011; 120:2938–2944.

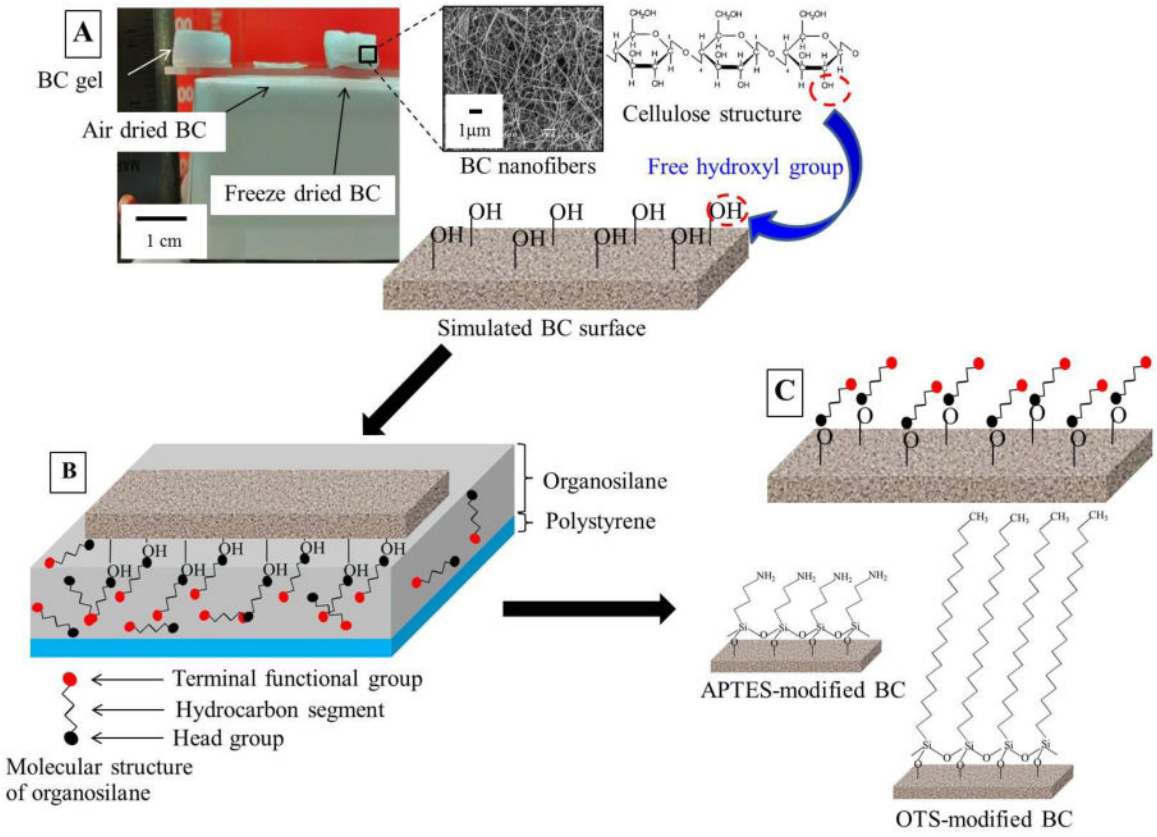

Fig. 1.

Illustration of modifying bacterial nanocellulose (BC) samples using organosilanes: 3-aminopropyltriethoxysilane (APTES) and octadecyltrichlorosilane (OTS), and the resulting idealized self-assembled monolayer on their surfaces. (A) BC samples were prepared by ambient-air drying for 48 h or freeze drying for 24 h. A surface of dried BC having abundant of hydroxyl groups was illustrated. (B) The BC surface was in contact with a thin layer (∼ 0.1 mm) of 1 wt.% organosilane/hexane solution on polystyrene Petri dish for 30 sec. Self-assembly of organosilane molecules formed by chemisorbing active head groups at the surface of BC. Loosely adsorbed molecules of organosilanes were removed by contacting the BC surface with a thin layer of silane-free hexane. (C) Organosilane-modified BCs (APTES- and OTS-modified BCs) were then dried with a stream of nitrogen gas, and annealed at 65 °C for an hour. Amine- and methyl-terminated BCs were ready for further characterizations.

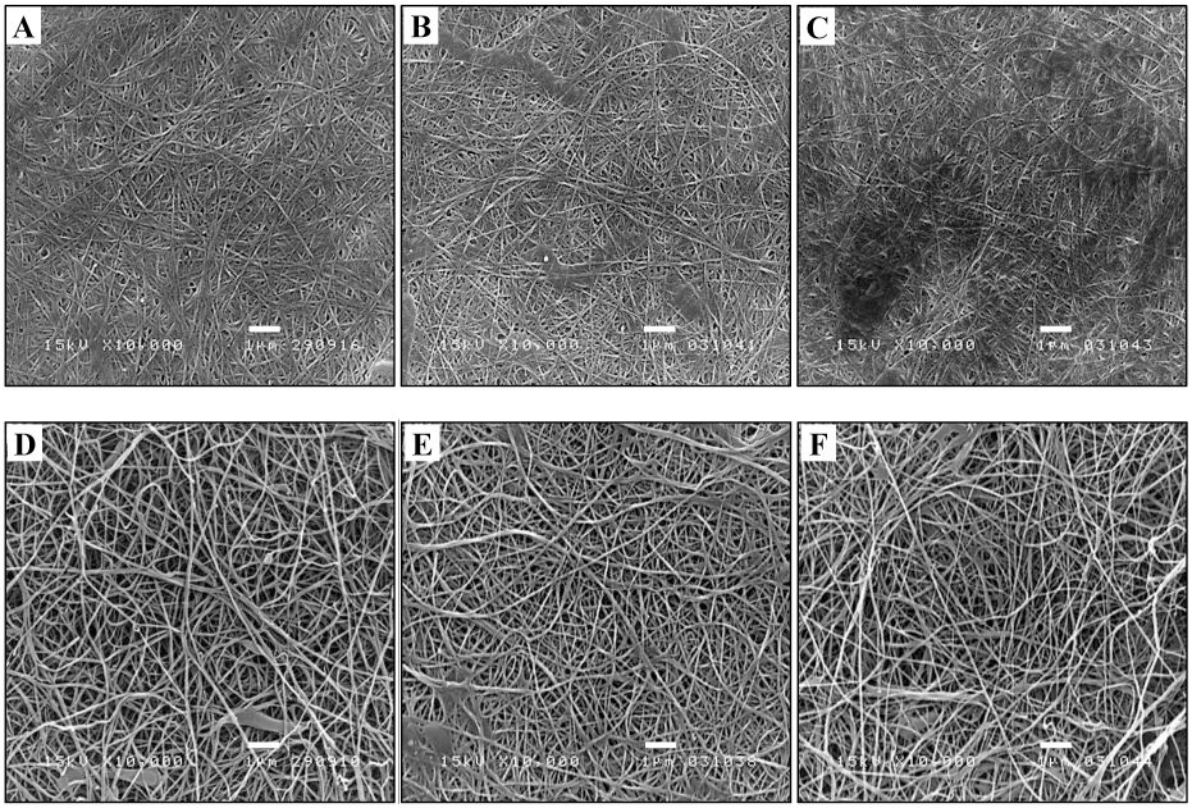

Fig. 2.

Typical SEM micrographs of surfaces of an air dried BC (A) and a freeze dried BC (D) and their corresponded surfaces functionalized using OTS (B and E) and APTES (C and F). The unmodified and modified BCs were scanned by SEM at a magnification of 10,000× and an accelerating voltage of 15 kV. The scale bars represent 1 μm.

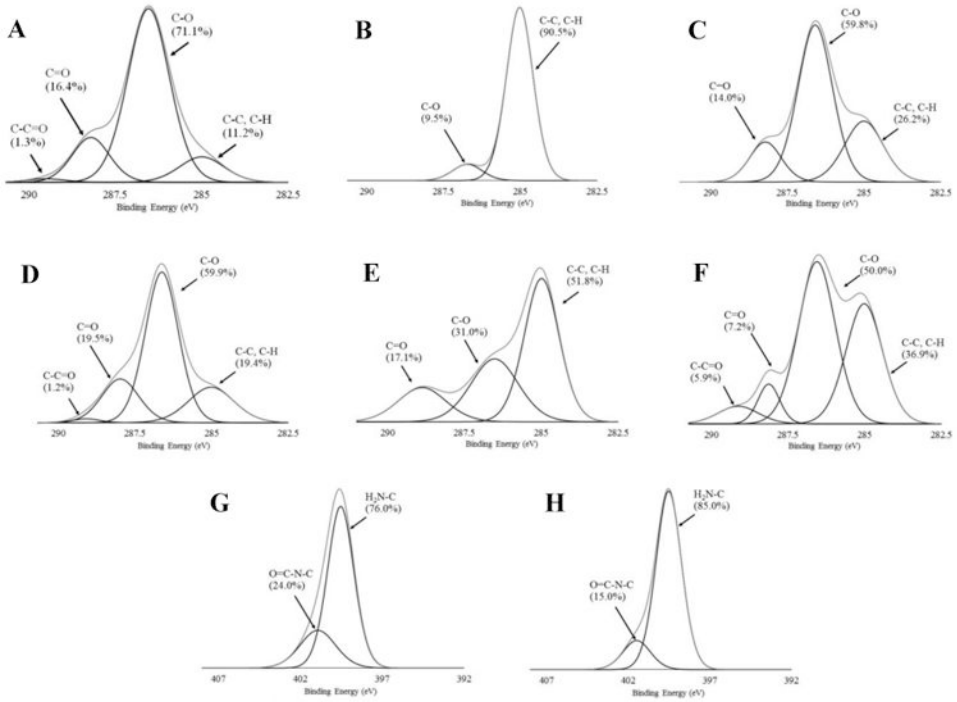

Fig. 3.

XPS high resolution C1s spectra of air dried BC (A), freeze dried BC (D), and their functionalized surfaces using OTS (B and E) or APTES (C and F), and N1s spectra of the APTES-modified air dried BC (G) and the APTES-modified freeze dried BC.

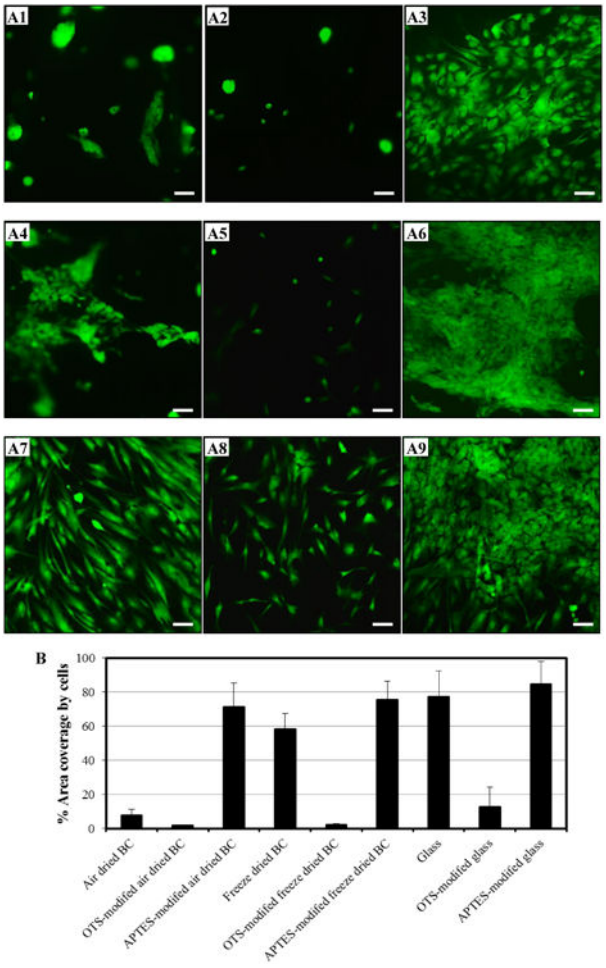

Fig. 4.

Representative fluorescence micrographs of attached and spread NHDF cells cultured on air dried BC (A1-A3), freeze dried BC (A4-A6), and glass slide (A7-A9). The incubation of NHDF cells was carried out on unmodified (A1, A4, and A7), OTS-modified (A2, A5, and A8), and APTES-modified (A3, A6, and A9) samples for 48h. Live NHDF cells (green) on the culture area of ~8×8 mm^2 were stained and captured using an Olympus IX70 microscope with 10× objective lens (the scale bar in each image is 100 μm). Visualized images were analyzed to obtained % area coverage by cells on the prepared surfaces (B) using color rage mode. 12 images from random locations of each sample were quantified. Results express as mean ± SD.

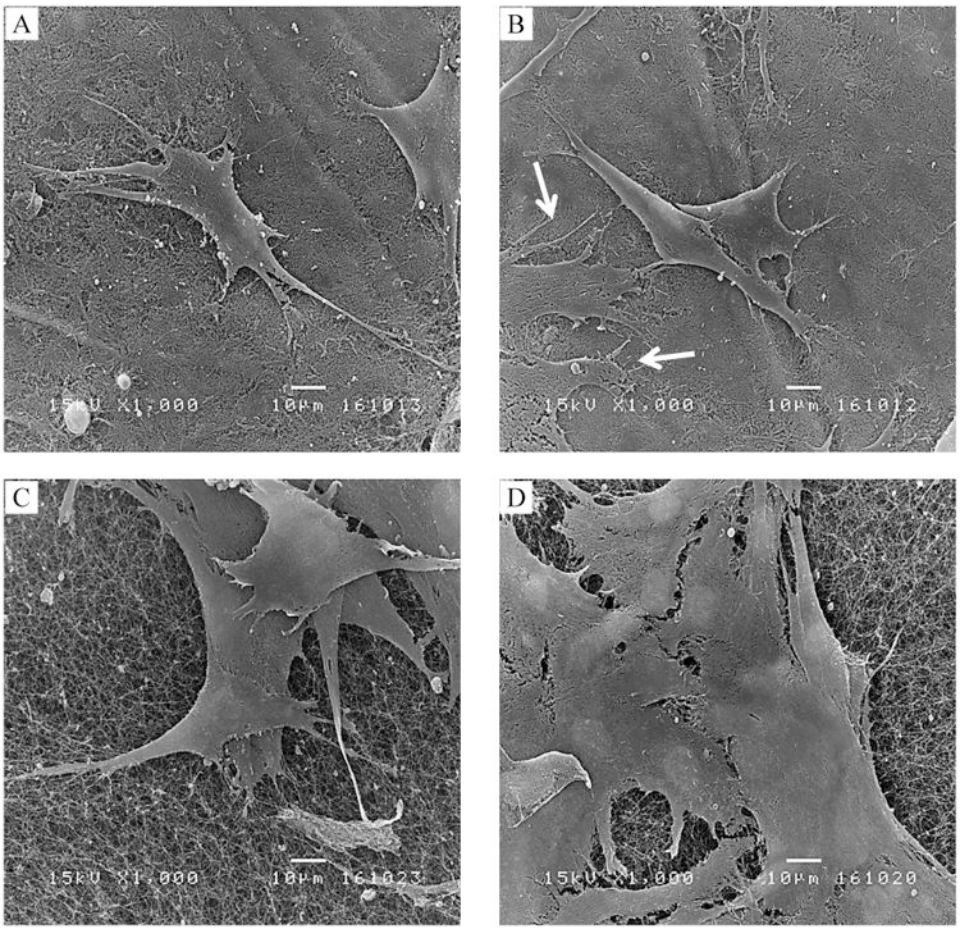

Fig. 5.

SEM micrographs of NHDF spreading on typical surfaces of an air dried BC (A) and a freeze dried BC (C), APTES-modified surfaces of air dried BC (B) and APTES-modified surfaces of freeze dried BC (D). After incubation for 48h, a greater spreading of NHDF cells appeared on APTES-modified BC as compared to unmodified BC was visualized at the magnification of 1000×. Arrows in (B) indicated the spreading of a cell. The fiber structures of air dried and freeze dried BCs could also be viewed underneath the cells. The scale bars represent 10 μm.

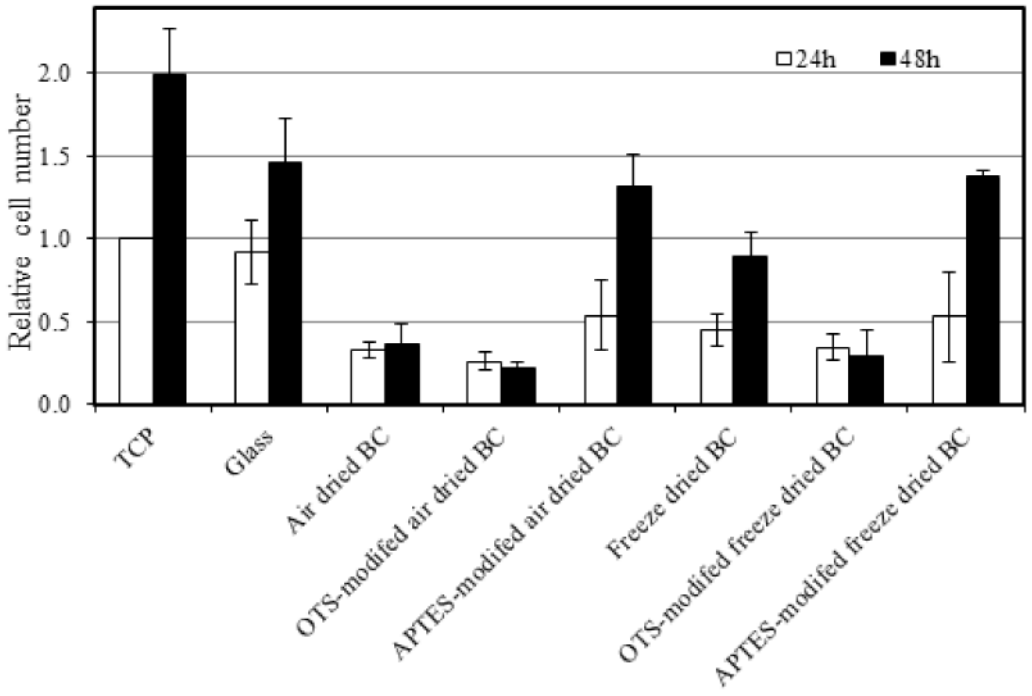

Fig. 6.

Relative NHDF cell numbers on different surfaces determined by MTT assay after 24 (white bar) and 48 h (black bar) of incubations. The *in vitro* experiments were independently performed in triplicate. The cell number in tissue culture polystyrene after 24 h of incubation was defined as 1.0. Results expressed are mean ± SD.

Table 1

Water contact angles (θ_w) on unmodified and organosilane-modified BCs. The contact angles were measured on at least four random locations of each sample, and the values were expressed as mean±SD

Samples	θ_W (°)
Air dried BC	56.3±8.0
Freeze dried BC	-
OTS-modified air dried BC	90.7±5.1
OTS-modified freeze dried BC	112.4±9.5
APTES-modified air dried BC	67.6±2.3
APTES-modified freeze dried BC	-

Table 2

Surface elemental composition and atomic ratio of BCs and modified BCs analyzed by XPS

Samples	Carbon (%)	Oxygen (%)	Nitrogen (%)	O/C	N/C
Air dried BC	51.5	47.4	0.5	0.92	0.009
Freeze dried BC	52.9	46.4	0.1	0.88	0.001
OTS-modified air dried BC	55.5	41.2	0.3	0.74	0.005
OTS-modified freeze dried BC	63.7	30.9	0.3	0.49	0.004
APTES-modified air dried BC	52.9	44.3	2.6	0.83	0.05
APTES-modified freeze dried BC	51.4	45.3	1.2	0.88	0.02